OPEN ACCESS

University of BRISTOL

Lizio, M. G., Andrushchenko, V., Pike, S. J., Peters, A. D., Whitehead, G. F. S., Vitórica-Yrezábal, I. J., Mutter, S. T., Clayden, J., Bouř, P., Blanch, E. W., & Webb, S. J. (2018). Optically Active Vibrational Spectroscopy of α-Aminoisobutyric Acid Foldamers in Organic Solvents and Phospholipid Bilayers. *Chemistry - A European Journal*, *24*(37), 9399-9408. https://doi.org/10.1002/chem.201801121

Peer reviewed version

Link to published version (if available):
10.1002/chem.201801121

Link to publication record in Explore Bristol Research
PDF-document

This is the author accepted manuscript (AAM). The final published version (version of record) is available online via Wiley-VCH at https://onlinelibrary.wiley.com/doi/abs/10.1002/chem.201801121 . Please refer to any applicable terms of use of the publisher.

University of Bristol - Explore Bristol Research

General rights

This document is made available in accordance with publisher policies. Please cite only the published version using the reference above. Full terms of use are available:
http://www.bristol.ac.uk/red/research-policy/pure/user-guides/ebr-terms/

Optically-Active Vibrational Spectroscopy of α-Aminoisobutyric Acid Foldamers in Organic Solvents and Phospholipid Bilayers

Maria Giovanna Lizio,[a,b] Valery Andrushchenko,[c]* Sarah J. Pike,[a,b,d] Anna D. Peters,[a,b] George F. S. Whitehead,[b] Iñigo J. Vitórica-Yrezábal,[b] Shaun T. Mutter,[a] Jonathan Clayden,[e] Petr Bouř,[c] Ewan W. Blanch,[f]* and Simon J. Webb[a,b]*

Abstract: Helical α-aminoisobutyric acid (Aib) foldamers show great potential as devices for the communication of conformational information across phospholipid bilayers, but determining their conformation in bilayers remains a challenge. In the present study, Raman, Raman optical activity (ROA), infrared (IR) and vibrational circular dichroism (VCD) spectroscopies have been used to analyze the conformational preferences of Aib foldamers in solution and when interacting with bilayers. A 3_{10}-helix marker band at 1665-1668 cm^{-1} in Raman spectra was used to show that net helical content increased strongly with oligomer length. ROA and VCD spectra of chiral Aib foldamers provided the chiroptical signature for both left- and right-handed 3_{10}-helices in organic solvents, with VCD establishing that foldamer screw-sense was preserved when the foldamers became embedded within bilayers. However, the population distribution between different secondary structures was perturbed by the chiral phospholipid. These studies indicate that ROA and VCD spectroscopies are valuable tools for the study of biomimetic structures, such as artificial signal transduction molecules, in phospholipid bilayers.

Introduction

Foldamers are synthetic oligomers that can fold into defined conformations, with long foldamers producing large well-defined surfaces that can interact with biopolymers or biomolecular assemblies.[1] Given these characteristics, there is much interest in applying foldamers to biomimetic chemistry and synthetic biology, for example to imitate protein–protein interactions,[2] to mimic signal transduction,[3,4] to produce DNA complexes for gene delivery,[5] to mimic cell-penetrating peptides[6] and to provide antimicrobial activity.[7,8,9] Of the different foldamer classes, those containing high proportions of α-aminoisobutyric acid (Aib) have a number of attractive features for applications as devices within membranes. These features include high hydrophobicity and an ability to adopt stable 3_{10}-helices, a conformation that is stabilized by Aib residues[10,11,12] and comprises sequences of three or more type III β-turns.[13] Aib foldamers in phospholipid bilayers form ion channels in a length dependent manner,[14] and show antibiotic activity[15] that may originate from their structural similarity to a naturally occurring class of antimicrobial peptide, the peptaibols. Peptaibols contain large proportions of Aib, which gives them a high propensity to fold into 3_{10}-helices.[10,16] Aib foldamers in 1,2-dioleoyl-*sn*-glycero-3-phosphocholine (DOPC) bilayers[3b,c] can relay (photo)chemical information over multi-nanometer distances,[3,4] using external stimuli to induce conformational switching between helical screw-senses. However, it is not yet established that an Aib foldamer maintains the same conformational preference in a DOPC bilayer as it does when dissolved in an organic solvent, and if 3_{10}-helices are still present whether they have the same absolute helical screw-sense.

In general, determining the folded structures of membrane-embedded oligomers, such as peptides, is a challenge. Unpolarized vibrational spectroscopies may provide some insight, as they are well-established for the investigation of protein and peptide secondary structure in solution, with conformational information principally found in the amide I (1620 cm^{-1} to 1680 cm^{-1}) and amide III (1200 cm^{-1} to 1400 cm^{-1}) regions.[17] However, these spectroscopies have not been widely applied to the study of 3_{10}-helical peptides in solution. The amide I maximum peak for 3_{10}-helix in infrared (IR) spectra is reported at 1662-1666 cm^{-1},[18,19] but this range is close to that for another helical secondary structure, α-helix, which is reported at 1650-1658 cm^{-1} and gives peaks with a similar spectral shape.[18,20,21,22,23] Other secondary structures give peaks in regions around 1633/1684 cm^{-1} (β-sheet), 1672 cm^{-1} (turns) and 1654 cm^{-1} (disordered).[22] Although some α-amino acid based polypeptides, such as $(Ala)_n$, can form 3_{10}-helices with a right-handed screw sense (the same sense as natural α-helices), these other conformations can compete. It has been reported that the length of the peptide, the proportion of Aib residues and

[a] Dr M. G. Lizio, Dr S. J. Pike, A. D. Peters, Dr S. T. Mutter, Dr S. J. Webb
Manchester Institute of Biotechnology, University of Manchester, 131 Princess St, Manchester M1 7DN, United Kingdom.
E-mail: S.Webb@manchester.ac.uk
[b] Dr M. G. Lizio, Dr S. J. Pike, A. D. Peters, Dr G. F. S. Whitehead, Dr I. J. Vitórica-Yrezábal, Dr S. J. Webb
School of Chemistry, University of Manchester, Oxford Road, Manchester M13 9PL, United Kingdom.
[c] Dr V. Andrushchenko, Prof. Dr. P. Bouř
Institute of Organic Chemistry and Biochemistry, Academy of Sciences, Flemingovo náměstí 2, 16610, Prague 6, Czech Republic.
E-mail: valery.andrushchenko@uochb.cas.cz
[d] Dr S. J. Pike
Faculty of Life Sciences, University of Bradford, Bradford, West Yorkshire, BD7 1DP, United Kingdom.
[e] Prof. Dr. J. Clayden
School of Chemistry, University of Bristol, Cantock's Close, Bristol BS8 1TS, United Kingdom.
[f] Prof. Dr. E. W. Blanch
School of Science, RMIT University, GPO Box 2476, Melbourne, Victoria 3001, Australia
E-mail: ewan.blanch@rmit.edu.au

Supporting information for this article is given via a link at the end of the document

the nature of the solvent can influence the equilibrium between 3_{10}-helix and α-helix.[24,25] For example, the best known peptaibol, alamethicin, folds into an α-helix with some 3_{10}-helical character at the C-terminus in the solid state,[26] a structure that NMR studies have shown is largely maintained in bilayers.[27,28,29]

a) **Achiral foldamers**

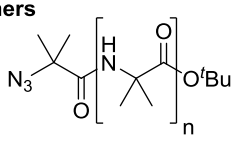

1 (n = 1); **2** (n = 3); **3** (n = 4); **4** (n = 5); **5** (n = 6); **6** (n = 7).

b) **Chiral foldamers**

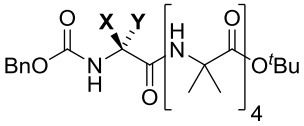

(***R***)**-7** (D-Phe cap, **X** = H, **Y** = CH_2Ph)
(***S***)**-7** (L-Phe cap, **X** = CH_2Ph, **Y** = H)

(***R***)**-8** (D-αMeVal cap, **X** = Me, **Y** = $CHMe_2$)
(***S***)**-8** (L-αMeVal cap, **X** = $CHMe_2$, **Y** = Me)

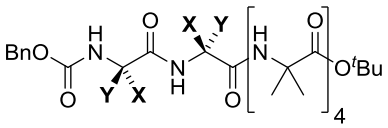

(***S***)**-9** ((L-αMeVal)$_2$ cap, **X** = $CHMe_2$, **Y** = Me)

c)

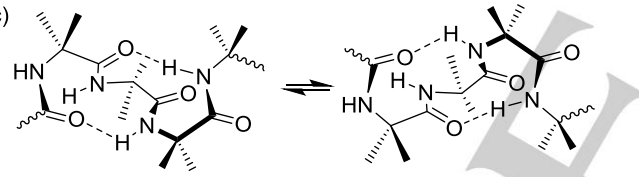

d)

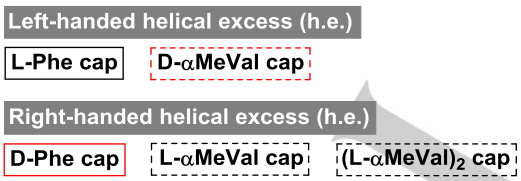

Figure 1. a) Chemical structures of the achiral foldamers **1**-**6** ($N_3Aib_nO^tBu$, n = 1, 3 to 7). b) Chiral foldamers (***R***)**-7**, (***S***)**-7**, (***R***)**-8**, (***S***)**-8**, and (***S***)**-9**. c) Equilibrium between left- and right-handed 3_{10}-helical conformations for Aib foldamers. d) Effect of different N-terminal caps on the distribution between left- and right-handed 3_{10}-helical conformations (the helical excess, h.e.). Also shown is the color coding used in spectra; black lines for L-amino acid caps, red lines for D-amino acid caps, full lines for Phe caps; dashed lines for αMeVal caps.

Optically active techniques, such as vibrational circular dichroism (VCD) and Raman optical activity (ROA), offer better ways to discriminate between α- and 3_{10}-helical conformations. Indeed, unlike IR, VCD spectroscopy can distinguish between α- and 3_{10}-helical conformations.[30,31] Crucially, both VCD and ROA should provide information about the absolute helical sense, which is especially important for foldamers and peptaibols with large proportions of achiral Aib but very few chiral residues. VCD studies have been performed on right-handed 3_{10}-helical peptides (negatively signed bands at ~1680 cm^{-1} and 1520 cm^{-1} and positive at ~1660 cm^{-1}),[31] but only one instance of ROA analysis of a 3_{10}-helical peptide has been reported: studies in water on a polar heptapeptide with a propensity to adopt a right-handed screw sense suggested a potential marker band for 3_{10}-helix secondary structure at 1668 cm^{-1} (with positive sign),[32] which was corroborated by theoretical modelling.[33]

To explore how this proposed 3_{10}-helix marker band could be exploited for the conformational analysis of Aib foldamers in different apolar environments (the reported ROA marker band was determined in water), we have performed Raman, ROA, IR and VCD spectroscopic studies on a series of homologous achiral foldamers and chiral derivatives (Figure 1 a,b). These studies aimed to show how optically active vibrational spectroscopies can determine both the relative proportion and chiral sense of 3_{10}-helical structure in Aib foldamers, both in organic solvents and bilayer membranes.

Results and Discussion

In the absence of a chiral group in the foldamer, racemic Aib foldamers exist as a mixture comprising equal populations of interconverting right-handed (*P*) and left-handed (*M*) 3_{10}-helices (Figure 1 c). Exchange between *M*- and *P*-helical conformations is fast on the NMR spectroscopy timescale, with a rate constant of *ca*. 1200 s^{-1} and an activation barrier per residue of 4.6 $kJ.mol^{-1}$.[34] Covalently or non-covalently appending a chiral group onto the N-terminus can bias the population distribution towards one helical conformation over the other; the extent of this bias is reflected in the helical excess (h.e.).[35] For example, NMR spectroscopy studies in organic solvents have shown that chiral quaternary L-amino acids bearing two different substituents at the α-carbon, such as L-α-methylvaline, at the N-terminus favor a right-handed helix.[12] In contrast, the opposite screw-sense preference is found for tertiary residues, such as L-Phe, at the N-terminus (Figure 1 d).[12] However, the use of NMR spectroscopy for conformational analysis is complicated by the need to make enantiopure ^{13}C labelled probes[36] or the need to use solid state NMR spectroscopy to characterize foldamers embedded in phospholipid bilayers.[3b]

Like the naturally occurring peptaibols, foldamers **1** to **9** have both N- and C- termini functionalized. These caps can modulate the stability of the 3_{10}-helix, e.g. a t-Bu ester induces formation of a destabilizing Schellman-like motif at the C-terminus of the peptides,[37] whilst an N-terminal Cbz ($PhCH_2OC(O)$) adds an extra hydrogen bond that can stabilize the 3_{10}-helix.[14b] Nonetheless, Aib foldamers with four residues or more form 3_{10}-helical structures even in the presence of destabilizing capping groups. Aib dimer **1** ($N_3Aib_2O^tBu$) is too short to form a helical structure,[37] whereas Aib tetramer **2** ($N_3Aib_4O^tBu$) adopts a 3_{10}-helical conformation in the solid state and appears to adopt the same conformation in organic solvents.[37] To confirm that the

longer foldamers **5** and **6** are folded into well-defined 3_{10}-helices,[38] the crystal structures of heptamer **5** ($N_3Aib_7O^tBu$) and octamer **6** ($N_3Aib_8O^tBu$) were determined (see the ESI). These structures confirmed that the compounds adopted homologous 3_{10}-helical conformations in the solid state (Figure 2), with both 3_{10}-helix screw-senses equally present in the unit cell. These 3_{10}-helices have four (for **5**) or five (for **6**) intramolecular hydrogen bonds running down the 3_{10}-helix axis (Figure 2), suggesting that the 3_{10}-helical conformation for these compounds should be more stable than that of tetramer **2**, which has a single hydrogen bond to maintain the helix.

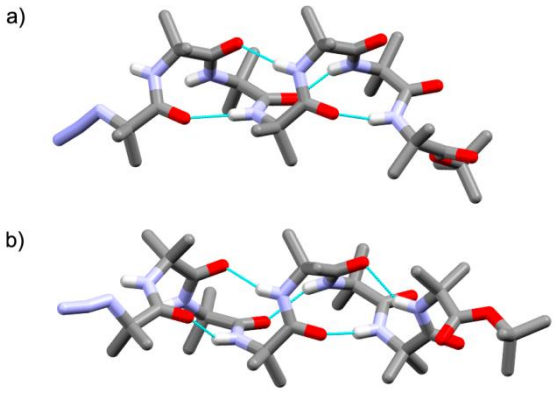

Figure 2. X-ray crystal structures of a) heptamer **5** ($N_3Aib_7O^tBu$) and b) octamer **6** ($N_3Aib_8O^tBu$) showing 3_{10}-helical conformations. Intramolecular hydrogen bonds are shown in cyan. Methyl and methylene hydrogens removed for clarity; grey = C, blue = N, red = O, white = H.

Raman spectroscopy of achiral Aib foldamers in organic solvents

Aib foldamers have a hydrophobic surface, which facilitates membrane insertion, so an organic solvent is needed to dissolve them. Chloroform, with a low dielectric constant (relative permittivity) of 4.81 and a dipole moment of 1.05 D, has often been used to mimic the low polarity found at the center of the bilayer.[39] However, if sealed cells are either not available or not suitable, the high volatility of chloroform may be a drawback for performing measurements that may take many hours, such as ROA and VCD. In addition, chloroform vibrational bands can interfere with those of the peptide. There is also the potential for intermolecular aggregation of longer foldamers at high concentrations typically required for ROA experiments (> 40 $mg.mL^{-1}$). $[D_6]$DMSO (non-deuterated DMSO has bands in the amide I region) is a lower volatility, higher polarity (dielectric constant 46.7, dipole moment of 3.96 D) alternative solvent that is a good hydrogen bond acceptor, weakening intermolecular interactions between foldamers.[40] Although this solvent is known to destabilize protein secondary structure[41] and has been reported to cause switching from 3_{10}- to α-helical conformations in peptides,[42] NMR spectroscopy studies of the octapeptide $CbzAib_5$(L-Leu)Aib_2OMe demonstrated that 3_{10}-helical conformations were preferred over α-helical conformations in $[D_6]$DMSO.[43] Therefore, both solvents were assessed to find the most versatile solvent for both Raman and ROA spectroscopic measurements. Foldamers $N_3(Aib)_nO^tBu$ **1-6** were synthesized, the solids dissolved in either $CHCl_3$ or $[D_6]$DMSO to give foldamer concentrations of 121 $mg.mL^{-1}$, then their Raman and ROA spectra recorded.

In $CHCl_3$, the amide I region for peptides **1** to **6** (Figure 3 a) showed that some compounds displayed broad peaks with clear asymmetry, suggesting the coexistence of multiple secondary structures in solution. The peaks were therefore deconvoluted, using resolution-enhancing methods such as second derivatives,[22,44] in order to identify and assign the contributing bands, which may provide quantitative information about the relative contributions of different secondary structures.[45] Band deconvolution on the amide I region of foldamers **1** - **6** (Figure 3 and Table 1) showed that there were two chief contributors in this region, at 1661-1668 cm^{-1} (band 1) and 1679-1692 cm^{-1} (band 2).

Table 1. Amide I frequencies (cm^{-1}) and relative integral intensities of the Raman spectra of $N_3(Aib)_nO^tBu$ foldamers **1** - **6**. n/a = not observed.

Foldamer	Amide I, band 1	Amide I, band 2	Solvent
1 (*n* = 2)	n/a	1681 (100 %)	$CHCl_3$
1 (*n* = 2)	n/a	1674 (91%), 1684 (9%)	$[D]_6$DMSO
2 (*n* = 4)	1667 (40%)	1688 (60%)	$CHCl_3$
2 (*n* = 4)	1662 (38%)	1685 (62%)	$[D]_6$DMSO
3 (*n* = 5)	1666 (27%)	1682 (59%), 1692 (14%)	$CHCl_3$
4 (*n* = 6)	1661 (27%)	1679 (73%)	$CHCl_3$
4 (*n* = 6)	1668 (90%)	1688 (10%)	$[D]_6$DMSO
5 (*n* = 7)	1666 (64%)	1680 (36%)	$CHCl_3$
6 (*n* = 8)	1688 (100%)	n/a	$CHCl_3$

The shortest foldamer, Aib dimer **1**, is too short to form the type III β-turn found in 3_{10}-helices and presents a single peak at 1681 cm^{-1} (100 %), with a further peak for the ester carbonyl at *ca*. 1730 cm^{-1}. However, tetramer **2**, which is long enough to form a single turn, revealed a shoulder at 1667 cm^{-1} and a main band at 1688 cm^{-1} (Figure 3 a, *n* = 4, ester peak at *ca*. 1730 cm^{-1}), with an approximate population distribution of 40% and 60%. Deconvolution of the amide I band for $N_3Aib_5O^tBu$ **3** revealed three components, at 1666, 1682 and 1692 cm^{-1}, whilst the amide I profile for $N_3Aib_6O^tBu$ **4** is formed by peaks at 1661 and 1679 cm^{-1} in a 27% to 73% ratio. $N_3Aib_7O^tBu$ **5** also presents two peaks in the same region (at 1666 cm^{-1} and 1680 cm^{-1}, in a 64% to 36% ratio), whereas $N_3Aib_8O^tBu$ **6** generates only one peak in the amide I region, at 1668 cm^{-1} (100%), even after band deconvolution. The Raman spectrum suggests that this peptide adopts a single conformation in $CHCl_3$, and comparison of these

data with the X-ray structure (Figure 2 b) allows us to assign the band at 1661-1668 cm^{-1} to the 3_{10}-helical conformation. The increase in the proportion of foldamer in a 3_{10}-helical conformation correlates with an increase in the number of intramolecular hydrogen bonds that maintain the helical structure. The structure of the conformation that gives the higher wavenumber band (band 2) is unclear, although the observation that Aib dimer **1** only gives the 1681 cm^{-1} band suggests that it arises from a predominantly unfolded state.

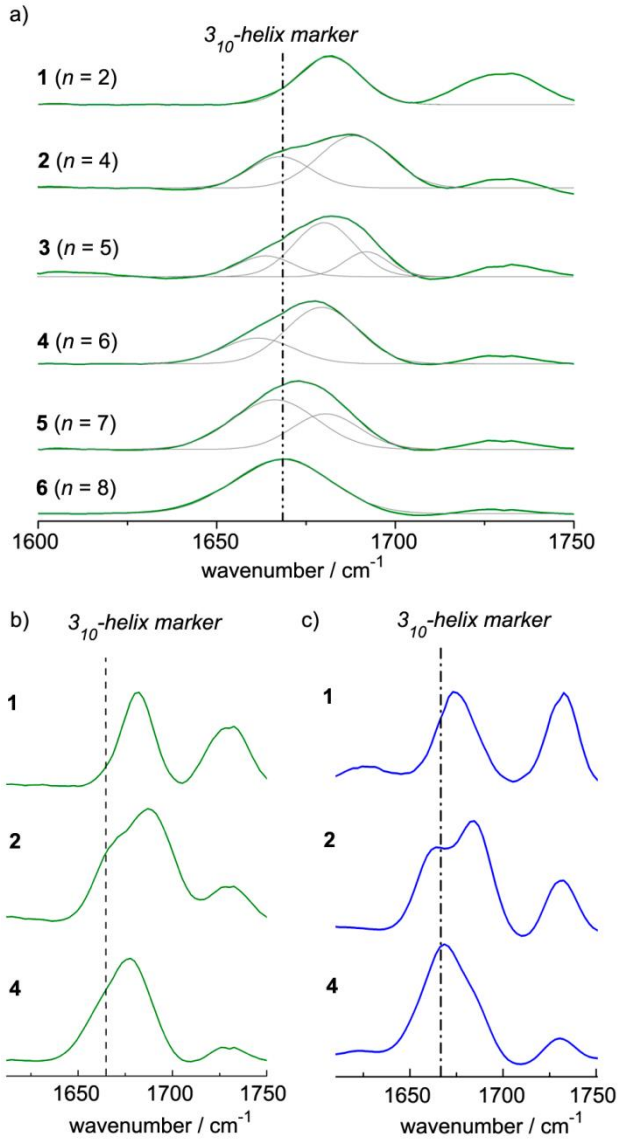

Figure 3. a) Experimental back-scattered Raman spectra for foldamers **1** - **6** ($N_3Aib_nO^tBu$, n = 2, 4-8) dissolved in $CHCl_3$. The amide I region is shown in each case. Peak deconvolutions are shown as gray traces. b,c) Comparison of the Raman spectra for foldamers **1**, **2** and **4** dissolved in either b) $CHCl_3$ (green traces) or c) [D_6]DMSO (blue traces). The amide I region is shown in each case. The vertical dotted line is at 1668 cm^{-1}, a wavenumber assigned to foldamers in a 3_{10}-helical conformation.

In [D_6]DMSO, the Raman spectra of **1**, **2** and **4** generally showed small differences (Figure 3 b,c) from those in $CHCl_3$. Foldamer **1** in $CHCl_3$ presents one maximum in the amide I region at 1681 cm^{-1}, whereas in [D_6]DMSO band deconvolution reveals the main peak at 1674 cm^{-1} with a shoulder at 1681 cm^{-1}. $N_3Aib_4O^tBu$ **2** dissolved in [D_6]DMSO showed a small shift to lower wavenumber in both deconvoluted bands compared to **2** dissolved in $CHCl_3$ with a negligible change in the population distribution (Table 1). The strongest influence from the solvent was observed for $N_3Aib_6O^tBu$ **4**. In $CHCl_3$, band deconvolution reveals the presence of a shoulder at 1661 cm^{-1} with a maximum peak at 1679 cm^{-1} (contributions of 27% and 73%, respectively). In [D_6]DMSO the amide I band is clearly different, with the maximum intensity now at 1668 cm^{-1} and a shoulder at 1688 cm^{-1}, with band deconvolution showing relative contributions of 90% and 10%, respectively. This observation suggests that despite the good hydrogen-bond accepting properties of this polar solvent, it does not destabilize 3_{10}-helical conformations and may even increase helical content when a peptide sequence is composed mainly of Aib residues; this observation is in agreement with NMR spectroscopic data reported for $CbzAib_5$(L-Leu)Aib_2OMe.[43]

Raman and ROA spectroscopy of chiral Aib foldamers in organic solvents

ROA spectroscopy is a technique that is highly sensitive to molecular chirality and structure, and has been used to discriminate between conformers of chiral compounds.[46,47,48] Although widely applied for the study of α-helical and β-sheet structures in proteins, there is only the 2004 report by Toniolo *et al* that describes an ROA spectroscopic investigation of a 3_{10}-helical peptide.[32] In general the most informative part of a peptide ROA spectrum is the amide III region,[22,46,49] which has a strong contribution from C_α-H deformations. However, this contribution is missing for quaternary amino acids, such as Aib, so the amide I region becomes a key region of ROA spectra for providing information about the secondary structure of peptides with high Aib-content or Aib foldamers.[32]

Aib foldamers **1** to **6** are achiral, so have equal amounts of interconverting (*P*) and (*M*) 3_{10}-helices.[34] However, adding a chiral cap, as in foldamers **(*R*)-7** and **(*S*)-7**, biases each equilibrium towards one helical screw sense and allows the foldamers to be detected using chiroptical spectroscopies. The chiral N-terminal phenylalanine "controller" cap in enantiomeric foldamers **(*S*)-7** and **(*R*)-7** causes the foldamer body to preferably adopt either a left-handed (*M*) helix (foldamer capped with Cbz(L-Phe)) or a right-handed (*P*) helix (foldamer capped with Cbz(D-Phe)) in organic solvents.[12] The extent of this bias is determined by the nature of the chiral capping group and can be quantified by using NMR spectroscopy to calculate the helical excess (h.e.), which for **(*R*)-7** is +40% (e.g. the *P*:*M* population ratio is 70%:30%).[35]

A valuable comparison with foldamers **(*R*)-7** and **(*S*)-7** is provided by foldamers **(*R*)-8** and **(*S*)-9**, which have either one or two chiral α-methylvaline (αMeVal) quaternary amino acid residues on the N-terminus. Chiral quaternary amino acid

residues at the N-terminus produce a type III β-turn and induce a helical screw sense opposite to tertiary amino acid controllers with the same configuration.[12] Therefore capping with D-αMeVal, as found in **(*R*)-8**, gives predominately the left-handed 3_{10}-helix, with an h.e. of −52% (*P*:*M* = 24%:76%). Inverting the configuration (to L-αMeVal) inverts the h.e. and adding a second L-αMeVal, as found in **(*S*)-9**, gives better control over the screw-sense preference, providing an h.e. of +72% (*P*:*M* = 86%:14%).[35] As well as providing a chiral influence, appending these residues to the Aib tetramer body can also stabilize the helix. The solid state structure of **(*rac*)-8** shows that adding a single Cbz-protected residue to the N-terminus of an Aib tetramer adds two intramolecular hydrogen bonds, to give three hydrogen bonds that stabilize the 3_{10}-helix.[14b]

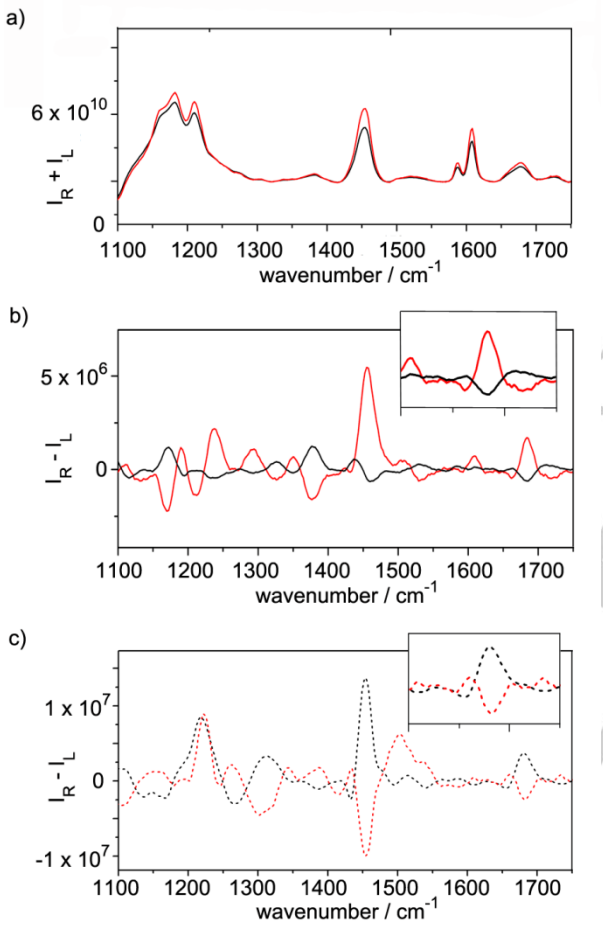

Figure 4. a) Raman and b) ROA spectra of foldamer **(*S*)-7** (L-Phe cap, left-handed helix, solid black line) and **(*R*)-7** (D-Phe cap, right-handed helix, solid red line). The measurements were carried out at 1.0 W in [D_6]DMSO for 48 h for each sample. Inset expands the region from 1600 to 1750 cm^{-1}. c) ROA spectra of foldamer **(*R*)-8** (D-αMeVal cap, left-handed helix, dashed red line) and **(*S*)-9** ((L-αMeVal)$_2$ cap, right-handed helix, dashed black line) in $CHCl_3$. Inset expands the region from 1600 to 1750 cm^{-1}.

Aib foldamers **(*R*)-7** and **(*S*)-7** were prepared separately by chemical synthesis, with the enantiomeric capping residues installed in the last synthetic step. The Raman and ROA spectra of **(*R*)-7** and **(*S*)-7** were recorded in [D_6]DMSO (Figure 4 a,b), with the aim of minimizing solvent evaporation and subsequent degradation of the samples caused by the strong laser irradiation over the 24-48 h course of a typical ROA acquisition. Each solution was photobleached in the cell before measurement (λ = 532 nm, *ca.* 2 h, laser power 600 mW at the sample) to remove any sample fluorescence. Since Raman spectroscopy is not sensitive to chirality, the Raman spectra of foldamers **(*R*)-7** and **(*S*)-7** show no significant difference (Figure 4 a). A strong peak is observed at 1630 cm^{-1}, which arises from the aromatic ring of phenylalanine,[50] and the band at 1454 cm^{-1} is assigned to an Aib side chain deformation vibration.[51,52] The amide I region presents a maximum at ~1680 cm^{-1} with a shoulder at 1664 cm^{-1}; the latter was attributed as a diagnostic signature band for 3_{10}-helical foldamer. The relatively strong intensity of the ~1680 cm^{-1} band suggests that these short foldamers, with only three intramolecular hydrogen bonds, are only partially folded into 3_{10}-helical structures.

The ROA spectra of the two enantiomers present mirror image features in the amide I region (Figure 4 b). The ROA spectrum of **(*S*)-7** (Cbz(L-Phe)Aib$_4$O^{t}Bu, *M* helix) shows very weak positively signed peaks at 1664 cm^{-1} and ~1710 cm^{-1}, with a stronger negatively signed peak at 1689 cm^{-1}, while foldamer **(*R*)-7** (Cbz(D-Phe)Aib$_4$O^{t}Bu, *P* helix) produces the mirror image (very weak negatively signed peaks at 1664 cm^{-1} and ~1720 cm^{-1}, with a stronger positively signed peak at 1689 cm^{-1}). The band at 1668 cm^{-1} has been assigned to peptides in a 3_{10}-helical conformation,[32] whereas the peak at 1689 cm^{-1} may arise from disordered secondary structures.[41] The amide I band for **(*S*)-7** and **(*R*)-7** appears distinct from an α-helix (right-handed) marker band, which is represented by a broad couplet that is negative at ~1640 cm^{-1} and positive at ~1665 cm^{-1}.[53,54] The compounds do not produce mirror image features in some other regions of the spectra, which could be due to differences in foldamer synthesis, sample preparation and sample treatment. The appearance of the amide I and II regions in the ROA spectra was reproducible, with artefacts due to birefringence excluded by repeated measurement of freshly prepared samples at different concentrations and on different ROA spectrometers (see ESI).

To confirm that the amide I signatures observed for **(*R*)-7** and **(*S*)-7** arose from their secondary structures, foldamers **(*R*)-8** and **(*S*)-9** were also chemically synthesized and studied. These spectra were recorded in $CHCl_3$ as the αMeVal-capped foldamers were found to be less susceptible to aggregation than **(*R*)-7** and **(*S*)-7**. Nonetheless, the high concentrations and the long acquisition times required for ROA data collection (between 24-48 h) caused some visible thermal decomposition of these analytes in this solvent; we found no particular advantages using $CHCl_3$ over [D_6]DMSO. Foldamer **(*R*)-8**, which has a D-αMeVal cap and should fold into a left-handed helix, showed the inverse spectral response to **(*R*)-7**, which has a D-Phe cap; the amide I region of **(*R*)-8** shows a positive peak at 1660 cm^{-1} and a negative peak at 1680 cm^{-1} (Figure 4 c). This observation suggests that this ROA signature arises from the secondary structure adopted by the foldamer rather than the configuration of the cap. The longer foldamer **(*S*)-9** (Cbz(L-αMeVal)$_2$Aib$_4$O^{t}Bu),

with two L-αMeVal residues in the cap, has a conformational population that is strongly biased towards right-handed helix. Indeed, this foldamer gives many bands of opposite sign to its pseudo-enantiomer **(*R*)-8**. However, the increase in the length of the foldamer, now with four intramolecular hydrogen bonds to stabilize the helix, did not strengthen the amide I signature from that observed for **(*R*)-8, (*R*)-7** and **(*S*)-7**.

The amide I signature for foldamer **(*R*)-7** (Cbz(D-Phe)Aib_4O^tBu, right-handed helix favored) is opposite in sign to that reported for a strongly right-handed 3_{10}-helical heptapeptide,[32] which in H_2O shows a small positive signed band at ~1668 cm^{-1}. Although **(*R*)-7** favors a right-handed helical conformation in solution (*P*:*M* ratio of 70:30 in $[D_4]CH_3OH$),[35] Raman studies on **1** – **6** revealed that for short foldamers, such as **7**, **8** and **9**, a significant conformational population that is not 3_{10}-helical may be present (up to ca. 75%). Analysis of the ROA spectra for these foldamers is therefore complicated by the weakness of the bands in the amide I region (perhaps exacerbated by oppositely signed contributions from the diastereomeric minor *M* conformer) and the presence of other conformations in solution that are not 3_{10}-helical but of unidentified structure.

We note that the ROA spectra of these foldamers will be from the ensemble of all of the dynamically interconverting conformations adopted in solution. Nonetheless, in the amide I region, mirror image ROA bands are reliably observed upon inversion of the 3_{10}-helical screw sense.

VCD spectroscopy of chiral Aib foldamers in organic solvents

VCD spectroscopy is a chiroptical spectroscopic technique that is complementary to ROA and has been used to study a number of Aib-containing peptides in organic solvents. Much like ROA, VCD allows comparison of spectroscopic signatures from α- and 3_{10}-helices. For example, studies of $CbzAib_n(L\text{-}Leu)Aib_2OMe$ (n = 0 to 5) in $CDCl_3$ solution carried out by Yasui *et al.* showed that the amide I band for an α-helix (right-handed) is negatively biased and intense while the amide I band for a right-handed 3_{10}-helix is only slightly positively biased and weak (negative at ~1680 cm^{-1}, and positive at ~1660 cm^{-1}).[40]

In this work, VCD analysis was performed on **(*R*)-7**, **(*S*)-7**, **(*R*)-8** and **(*S*)-8** in $[D_6]$DMSO. The relative intensity and position of the amide I and amide II bands in VCD spectra can be used to distinguish between α-helical and 3_{10}-helical secondary structures. For α-helix, the amide II band is significantly shifted from its absorption band and has lower intensity and larger bandwidth compared to amide I couplet.[18,55] On the other hand, the amide II band for 3_{10}-helix is situated much closer to its corresponding absorbance peak, is relatively sharp and has similar or larger intensity compared to the amide I couplet. Inspection of the VCD spectra of **(*R*)-7**, **(*S*)-7**, **(*R*)-8** and **(*S*)-8** showed all foldamers had fairly sharp and strong amide II bands, which suggests that a significant proportion of these foldamers adopts a 3_{10}-helical conformation. Multiple measurements on fresh solutions of **(*R*)-7** were performed to confirm the characteristic features in the spectra (e.g. amide II band shape and sign) were reproducible. The αMeVal-capped peptides **(*S*)-8** and **(*R*)-8** seem to have a higher proportion of 3_{10}-helix and/or a greater helical excess than the Phe-capped peptides **(*S*)-7** and **(*R*)-7**, as their amide II VCD signal is slightly more intense than their amide I VCD signal and the bands are less shifted from their corresponding absorbance bands than in the case of (12-19 cm^{-1} *vs*. 15-22 cm^{-1} respectively) (Figure 5).

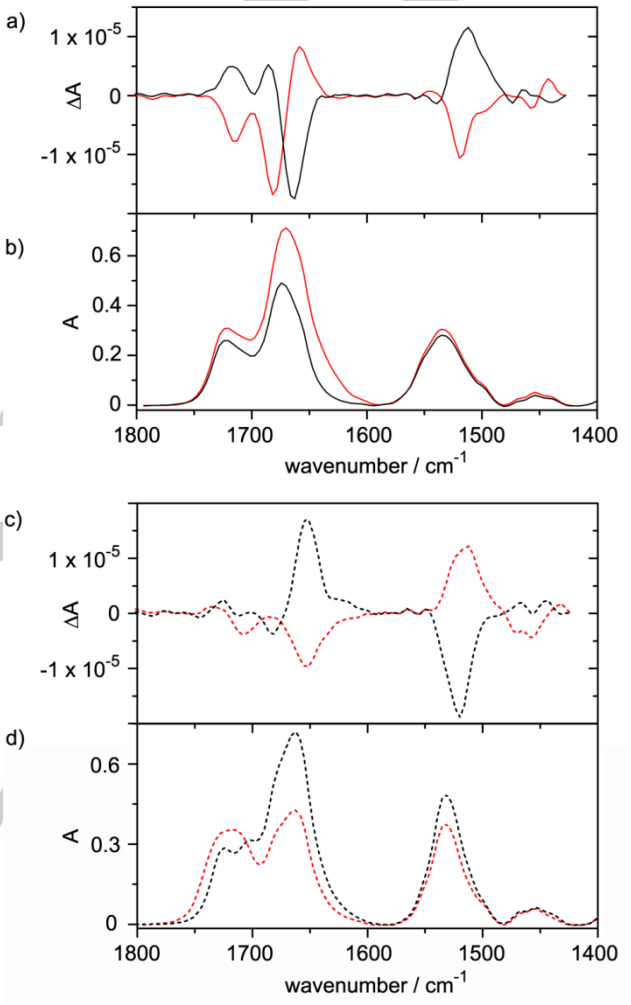

Figure 5. a) VCD spectra of **(*S*)-7** (L-Phe cap, left-handed helix, solid black line), **(*R*)-7** (D-Phe cap, right-handed helix, solid red line) in $[D_6]$DMSO; b) Corresponding IR spectra of **(*S*)-7** and **(*R*)-7** in $[D_6]$DMSO. c) VCD spectra of **(*R*)-8** (D-αMeVal cap, left-handed helix, dashed red line), **(*S*)-8** (L-αMeVal cap, right-handed helix, dashed black line) in $[D_6]$DMSO; d) Corresponding IR spectra of **(*R*)-8** and **(*S*)-8** in $[D_6]$DMSO. The difference in absorbance between enantiomers is ascribed to small variations in sample concentration and/or the pathlength of the dismountable VCD cell.

The VCD spectrum of $Cbz(L\text{-}Phe)Aib_4O^tBu$ **(*S*)-7** is dominated by the negative amide I couplet at 1664(-)/1685(+) and the positive amide II band at 1512 cm^{-1}, with corresponding absorption bands at 1674 and 1534 cm^{-1}, respectively (Figure 5 a,b). The VCD spectrum of Cbz(L-Phe)OH indicates that the positive VCD signal at 1718 cm^{-1} and the absorption band at

1722 cm^{-1} arise from the chiral Cbz(L-Phe) cap (see the ESI). The peptide with the opposite configuration of the cap, Cbz(D-Phe)Aib_4O^tBu **(*R*)-7**, shows nearly a mirror image VCD spectrum, but differences in sample preparation and treatment may produce spectral asymmetry, as well as experimental artefacts produced during these challenging measurements. Since the VCD spectra of both Cbz(L-Phe)OH and Cbz(D-Phe)OH show no bands below 1700 cm^{-1} (see the ESI), the spectral features between 1700 and 1500 cm^{-1} give information on the secondary structure adopted by the Aib oligomers. Bearing in mind that the VCD spectral shape is dependent on the relative contributions from interconverting diastereomeric conformations (a cap of fixed chirality followed by an *M* or *P* helical foldamer body), the sign of the amide I and II VCD bands is consistent with a predominance of left-handed 3_{10}-helix for **(*S*)-7** and right-handed 3_{10}-helix for **(*R*)-7**, respectively.[18,55]

Replacement of the Cbz(L-Phe) cap of **(*S*)-7** with the chiral quaternary amino acid Cbz(L-αMeVal) (to give **(*S*)-8**) will invert the screw sense of the helix, despite the cap having the same absolute configuration. Thus, the VCD spectrum of **(*S*)-8** (Cbz(L-αMeVal)Aib_4O^tBu) shows a positive amide I couplet at 1653(+)/1683(-) and negative amide II band at 1520 cm^{-1}, possibly arising from the IR bands at 1663 and 1532 cm^{-1}, respectively (Figure 5 c,d). Such a VCD pattern corresponds to right-handed helix, while the mirror-image VCD of **(*R*)-8** (Cbz(D-αMeVal)Aib_4O^tBu) corresponds to left-handed helix;[18,55] both observations are in agreement with x-ray crystallography and NMR spectroscopy studies.[12] The inverse spectral relationship between foldamers capped with Phe and αMeVal of the same configuration confirms that VCD bands in the amide I and amide II regions are reporting on the conformation of the foldamer rather than the chirality of the cap.

VCD spectroscopy of chiral Aib foldamers in phospholipid bilayers

The study of Aib foldamer conformation in membranes has recently become of keen interest in the area of artificial signal transduction,[3,56] with reports that conformational interchange of screw-sense in 3_{10}-helical Aib foldamers can be used to communicate photochemical or chemical signals over multi-nanometer distances deep into bilayers. These Aib foldamers were embedded within vesicles composed of DOPC, which gives very fluid bilayers that are commonly used for NMR studies of membrane-associated proteins.[57] How the bilayer affects Aib foldamer conformation is unclear, although the assumption has been made that a 3_{10}-helical conformation is still formed, with its helical sense the same as in solution.[3c] Indeed, solid state NMR spectroscopic analysis of alamethicin in DMPC bilayers has shown that this peptaibol largely retains its conformation in the bilayer when compared to the x-ray crystallographically determined structure.[26,58]

It was hoped that VCD analysis would provide some insight into the conformations adopted by chiral Aib foldamers when they are embedded in DOPC bilayers, although VCD has only infrequently been applied to the study of peptides in phospholipid bilayers.[59] Several different sizes of DOPC vesicle were assessed for their suitability for VCD analysis, including giant unilamellar vesicles and large unilamellar vesicles, both of which proved to be unsuitable. However, small unilamellar vesicles (SUVs) produced through sonication were found to give stable suspensions over the lifetimes of the VCD measurements without causing too many artefacts in the spectra. The spectrum of each foldamer/lipid suspension was measured immediately after sample preparation to minimise the effect of changes in sample composition over time, for example due to foldamer reorganisation in the bilayer, vesicle sedimentation and bilayer fusion. For this reason spectral averaging for each sample was not carried out, with measurements on fresh samples performed instead.

The VCD and IR spectra of DOPC SUVs without foldamer revealed a window from 1700 to 1500 cm^{-1}, which is free of strong IR peaks (e.g. lipid C=O stretching at ~1725 cm^{-1} and lipid CH_2 bending at ~1460 cm^{-1}) and VCD bands from the chiral glycerol group of DOPC (Figure 6 a,b). DOPC SUVs containing foldamers **(*S*)-7** and **(*R*)-7** (lipid:foldamer weight ratio of 4.4:1) were prepared in deuterated PBS buffer (PBS salts reconstituted in D_2O, pD 7.4).

The IR spectrum of **(*S*)-7** (Cbz(L-Phe)Aib_4O^tBu, *M* helix) in DOPC SUVs showed a complex amide I' pattern with three distinct peaks at 1694, 1671, 1651 cm^{-1} (Figure 6 d, amide I' denotes an amide I band from peptide in deuterated solvent). There is an amide II band at 1520 cm^{-1}, and despite being close to a DOPC band, an amide II' band (for deuterated foldamer) that is clearly distinguishable at 1431 cm^{-1} on the low-wavenumber shoulder of the lipid CH_2 bending mode. A combination of amide II and amide II' bands has been observed before for other peptides embedded in lipid bilayers and possibly occurs due to incomplete hydrogen-deuterium exchange of the amide NH groups.[59d,e]

For both foldamers **(*S*)-7** and **(*R*)-7** in bilayers, the intensity of the VCD signal was significantly higher (5-10 fold) in the bilayer than for the foldamers in [D_6]DMSO (see the ESI), which could mean that either they become more rigid in the bilayer or the helical excess significantly increases (or both of these factors). Furthermore, the combined intensity of amide II and amide II' VCD bands is similar to (for **(*R*)-7**) or higher than (for **(*S*)-7**) the amide I' VCD intensity, while the bands are sharp and their position almost coincides with the corresponding IR absorption peaks (within a few cm^{-1}). These observations imply that foldamer in a bilayer could have a higher 3_{10}-helical content than when in [D_6]DMSO.

Foldamer **(*S*)-7** showed a complex amide I' pattern in the VCD spectrum (Figure 6 c), with a positive peak at 1695 and negative peaks at 1668 and 1655 cm^{-1}. The complex VCD pattern and multiple IR peaks in the amide I' region seem to suggest partitioning of the peptides into a few (two to three) conformational subgroups, producing bands that are a combination of bands or couplets from all the individual subgroups. If we assume that the IR peaks are related to the foldamer conformations (and not to foldamer-lipid interactions), then we suggest the following assignments: the peaks at 1651-1652 cm^{-1} arise from α-helix, bands at 1671-1673 cm^{-1} correspond to 3_{10}-helix and those at 1694-1696 cm^{-1} originate

from bends and turns.[23,60] The amide II and amide II' vibrations gave rise to positive VCD bands at 1523 and 1432 cm^{-1}, respectively. The positive sign of these bands indicates that foldamer **(*S*)-7** in the bilayer adopts a left-handed helical structure, as found for **(*S*)-7** in organic solvent.

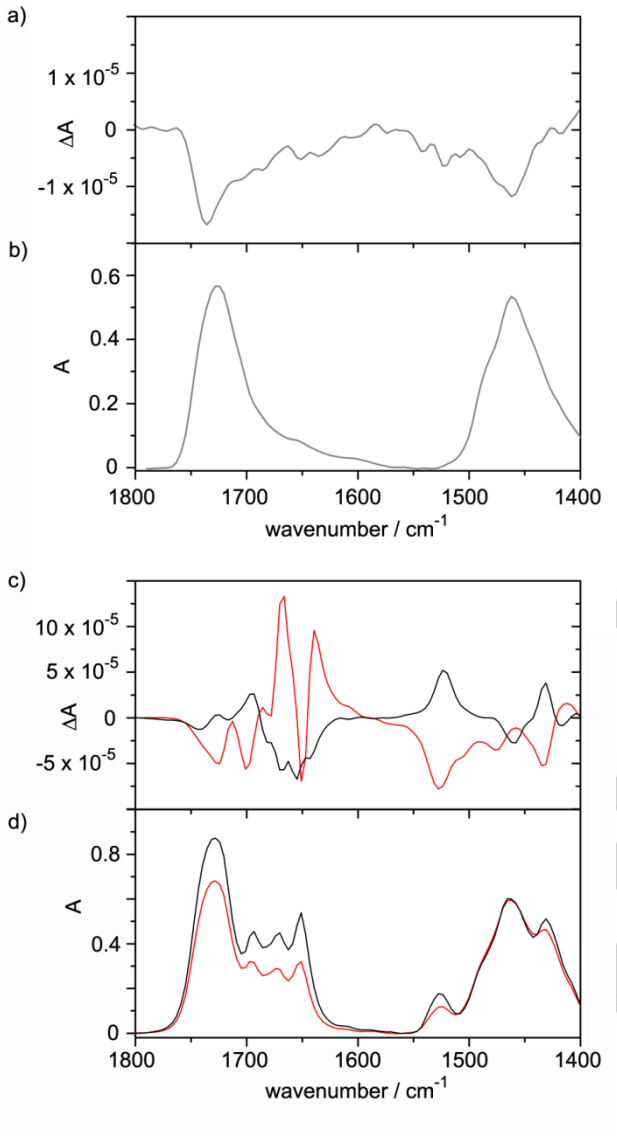

Figure 6. a) VCD spectrum of blank DOPC SUVs in PBS/D_2O; 220 $mg.mL^{-1}$; 50 μm path length; BaF_2 cell; 29 °C (grey trace). b) Corresponding IR spectrum of blank DOPC SUVs in PBS/D_2O. (c-d) Foldamers (50 $mg.mL^{-1}$) in SUVs (220 $mg.mL^{-1}$ DOPC). c) VCD spectra of **(*R*)-7** (red line) and **(*S*)-7** (black line) in DOPC vesicles. d) Corresponding IR spectra of **(*R*)-7** (red line) and **(*S*)-7** (black line) in DOPC vesicles.

In keeping with the complexity observed for **(*S*)-7**, the amide I' VCD spectrum recorded for the enantiomer **(*R*)-7** shows several bands with opposite sign (negative peak at 1700 and positive at 1668 cm^{-1}). However, the band at 1650 cm^{-1} remained negative (Figure 6 c), so the overall amide I' spectral shape does not appear as a mirror image of the corresponding region for **(*S*)-7** (1630-1700 cm^{-1}). This could occur due to the chiral membrane environment producing different helical excesses for these enantiomeric foldamers, resulting in different overlap of the individual spectral components. However this mixture could only be measured once, so experimental artefacts arising from the foldamer-containing vesicles themselves or the high sample absorption in this region might also contribute to the spectral asymmetry.

For **(*R*)-7**, the sense of the amide II and amide II' VCD bands at 1527 and 1433 cm^{-1}, respectively, is inverted compared to **(*S*)-7**. The negative sign of these bands suggests an excess of the right-handed helical structure for **(*R*)-7**. Therefore, the helical screw-sense of both foldamers in the lipid bilayer remains the same in DOPC bilayers as in $[D_6]DMSO$ solution. Thus, analytical studies of Aib foldamer conformation in organic solvents can be valuable model systems for studies in bilayers, which is a much more challenging environment for quantitative analysis.

Conclusions

The Raman spectra of Aib foldamers in organic solvents show a band at 1661-1668 cm^{-1} that proportionally increases in intensity with increasing foldamer length (dimer to octamer), while a band between 1679 and 1688 cm^{-1} decreases in intensity. For example, an Aib dimer that is too short to fold did not show any bands at ~1665 cm^{-1} but an Aib octamer that crystallized as a 3_{10}-helix gave a feature in the ~1665 cm^{-1} region almost exclusively. We propose that the Raman band at ~1665 cm^{-1} results from 3_{10}-helical conformations, whereas the Raman band at ~1684 cm^{-1} arises from poorly structured unfolded conformations. Although 3_{10}-helical content increases strongly with the length of Aib_n foldamers, to nearly 100% when n = 8, Raman spectroscopy can only show the fraction of peptide that is in a 3_{10}-helical conformation without any information regarding the helical sense. Screw-sense inversions (tendril perversions)[61] can still occur in the helix between 3_{10}-helical regions of opposite sense without significantly affecting overall 3_{10}-helix content.

ROA spectra were obtained for chiral Aib foldamers in organic solvents for the first time, identifying an amide I signature for partially 3_{10}-helical Aib tetramers in organic solvent. The ROA spectra of foldamers with different N-terminal chiral caps showed the sign of the ROA spectral bands reported on foldamer screw-sense rather than the configuration of the N-terminal controller. These studies suggest ROA could be a useful method for investigations of the conformation and stability of lipophilic peptaibols in organic solvents, although problems with solvent band interference and measurement reproducibility remain to be solved.

VCD spectroscopy of chiral Aib foldamers in $[D_6]DMSO$ showed that the sign of the VCD bands also reported on the foldamer screw-sense rather than on the configuration of the N-terminal controller. Since it was known that N-terminal L-Phe and D-αMeVal both induce a left-handed 3_{10}-helical

conformation,[12] we were able to show that this screw-sense resulted in a negative amide I VCD couplet in the 1650-1690 cm^{-1} range and a strong sharp positive amide II band at ~1520 cm^{-1} (with the respective enantiomers showing the converse). These findings correlate with earlier VCD studies on right-handed 3_{10}-helical peptides.[31]

We were also able to obtain IR and VCD spectra of tetrameric Aib foldamers capped with either L- or D-Phe in the membranes of vesicles at a relatively high loading of 20 wt %. The VCD data implies that partitioning into a bilayer increases the proportion of foldamer with 3_{10}-helical structure, and is also consistent with an increase in foldamer rigidity and/or helical excess. The sign of a 3_{10}-helix marker band at 1520 cm^{-1} is the same as the sign found in $[D_6]$DMSO, suggesting that the overall screw-sense preference of an Aib foldamer in organic solvent is retained even after the foldamer partitions into a DOPC lipid bilayer. The enantiomers did not give mirror image spectra within the 1580-1680 cm^{-1} window, and a question remains as to the cause of these observed differences in the amide I region. We suggest either the measurement produced unwanted artefacts, most probably due to sample aggregation or diminished instrumental sensitivity, or the chiral DOPC lipid perturbed the screw-sense equilibrium differently for each enantiomeric foldamer. Further investigations are continuing into the effect of phospholipid chirality on the conformation of Aib foldamers embedded in bilayers.

Experimental Section

Peptides **1** to **9** were synthesized according to previously published procedures.[14b,37] All samples were re-purified by high-performance liquid chromatography (HPLC) on an Agilent (Santa Clara, California, United States) 1100 series HPLC equipped with a semi-preparative C-18 column (Agilent Eclipse XDB-C18, 5 µm, 9.4 mm × 250 mm).

Single crystals of either $N_3Aib_7O^tBu$ **5** or $N_3Aib_8O^tBu$ **6** suitable for X-ray diffraction analysis were grown by slow diffusion of diethyl ether into a saturated solution of either **5** in chloroform at 23 °C or **6** in chloroform at 4 °C, respectively. X-ray crystallography details are reported in the Supporting Information. Structural data for **5** and **6** have been deposited with the Cambridge Crystallographic Data Centre. CCDC 1820749 and 1820749 contain the supplementary crystallographic data for **5** and **6** respectively. These data can be obtained free of charge from The Cambridge Crystallographic Data Centre via www.ccdc.cam.ac.uk/data_request/cif.

The vesicle samples for the VCD experiments were obtained by combining the appropriate amount of lipid (DOPC) from a stock solution (20 $mg.mL^{-1}$ in chloroform) with the corresponding amount of foldamer dissolved in spectroscopic grade chloroform (4 % molar ratio) in a 5 mL round-bottomed flask. The chloroform was removed under reduced pressure using a rotary evaporator until a thin film was formed on the walls of the flask. The film was further dried under high vacuum for at least 2 h. Deuterated Dulbecco's solution was freshly prepared by removing the water from commercially available Dulbecco's solution and rehydrated with deuterated water. Drying then resuspension in D_2O was repeated three times, and the buffer solution was used without further treatment. The deuterated Dulbecco's phosphate buffered saline solution (1 mL) was added to the flask and the lipid film was resuspended by vortex mixing, then sonicated at room temperature with a sonicator bath; samples were freshly prepared before analysis. The final total concentration of lipids was around 220 $mg.mL^{-1}$ in Dulbecco's solution (1 mL) and the final foldamer concentration was 50 $mg.mL^{-1}$. Spectra were measured immediately after sample preparation.

The Raman and ROA spectra of the samples in organic solvents were measured at a concentration of 121 $mg.mL^{-1}$. The samples were prepared by dissolving the solid material in $[D_6]$DMSO or $CHCl_3$. The samples were transferred into a 200 µL quartz micro-fluorescence cell. Each sample was photobleached (532 nm laser for *ca*. 2 h, laser power 600 mW at the sample) before measurement to until any fluorescence was removed. After complete removal of the fluorescence the Raman spectra were acquired.. The experiments were performed using a Chiral Raman-2X ROA spectrometer (BioTools, Inc., USA) operated using Critical Link (USA) software equipped with a Millennium Pro Nd-VO_4 laser (UK) at 532 nm excitation wavelength, laser power 600 mW at the sample, and spectra resolution of 7 cm^{-1}. The spectral acquisition time was 42 h. To confirm reproducibility of key spectral features in the amide I and II regions, data was collected on samples of **(*S*)-7** and **(*R*)-7** at a range of concentrations (53 to 121 $mg.mL^{-1}$ at 22 °C in temperature-controlled cells) on two different ROA spectrometers (in Prague and Manchester).

The IR and VCD measurements were performed upon the samples extracted from the ROA cell after Raman/ROA experiments. The foldamer samples in $[D_6]$DMSO were diluted to 40-50 $mg.mL^{-1}$. The samples of DOPC and foldamer-DOPC suspensions were prepared in D_2O-based PBS buffer as described above at concentrations of 220 $mg.mL^{-1}$ of DOPC and 50 $mg.mL^{-1}$ of the peptide to keep the lipid:foldamer weight ratio in the final mixture at *ca.* 4:1. The samples were placed in a dismountable BaF_2 VCD cell with a pathlength of 50 µm. The differences in the pathlength of the dismountable VCD cell, and/or small variations in the sample concentration can produce variations in sample absorbance. The IR and VCD spectra were acquired with the Chiral IR-2X VCD spectrometer (BioTools, Inc., USA) at 8 cm^{-1} resolution for 18 h. To avoid cell and baseline artefacts, solvent spectra were measured in the same cell under the same conditions as the samples and subtracted from the sample spectra, after which baseline correction was performed. Spectra of foldamer solutions were measured once per sample, with multiple measurements on **(*R*)-7** performed to confirm that characteristic spectral features were reproducible. Spectra of foldamer-DOPC suspensions were measured once per sample, over several hours in 30 minute slots, then averaged to give the final spectrum.

Raman and ROA spectra were processed using MATLAB 2010 software and an in-house toolbox. Conventional Raman spectra were baseline-corrected according to the method proposed by Eilers *et al*.[62] The ROA spectra were baseline corrected using a 80 point median filter and smoothed using a 15 point Savitzky-Golay filter. Spectral deconvolutions were carried out in OriginPro 9 using the inbuilt peak fitting and deconvolution tool; the area under peaks was measured to obtain integral intensities, with second derivatives used to calculate the peak centers. The second derivatives were Gaussian peaks iteratively fitted until convergence criteria were satisfied. All data were plotted using Origin 8.1 Pro software (OriginLab, USA).

Acknowledgements

Financial support from the BBSRC (BB/I007962 for SJP, SJW and JC; DTP PhD studentships for MGL), the EPSRC (EP/G03737X/1 and EP/N009134/1 for SJW), and the Czech

Science Foundation (grants 16-04902S for VA and 16-05935S for PB) is gratefully acknowledged.

Keywords: foldamers • peptides • vibrational spectroscopy • chirality • membranes

[1] C. M. Goodman, S. Choi, S. Shandler, W. F. DeGrado, *Nat. Chem. Biol*. **2007**, *3*, 252–262.
[2] V. Azzarito, K. Long, N. S. Murphy, A. J. Wilson, *Nat. Chem*. **2013**, *5*, 161–173.
[3] a) R. A. Brown, V. Diemer, S. J. Webb, J. Clayden, *Nature Chem*. **2013**, *5*, 853-860; b) M.; De Poli, W.; Zawodny, O.; Quinonero, M.; Lorch, S. J.; Webb, J., Clayden, *Science*, **2016**, *352*, 575-580; c) F. G. A.; Lister, B. A. F.; Le Bailly, S. J.; Webb, J., Clayden, *Nat. Chem*. **2017**, *9*, 420–425.
[4] L. Byrne, J. Solà, T. Boddaert, T. Marcelli, R. W. Adams, G. A. Morris, J. Clayden, *Angew. Chemie. Int. Ed.* **2014**, *53*, 151-155; *Angew. Chem*. **2014**, *126*, 155-159.
[5] J. E. Murphy, T. Uno, J. D. Hamer, F. E. Cohen, V. Dwarki, R. N. Zuckermann, *Proc. Natl. Acad. Sci. U. S. A.* **1998**, *95*, 1517–1522.
[6] A. D. Bautista, C. J. Craig, E. A. Harker, A. Schepartz, *Curr. Opin. Chem. Biol*. **2007**, *11*, 685–692.
[7] P. Claudon, A. Violette, K. Lamour, M. Decossas, S. Fournel, B. Heurtault, J. Godet, Y. Mély, B. Jamart-Grégoire, M.-C. Averlant-Petit, J.-P. Briand, G. Duportail, H. Monteil, G. Guichard, *Angew. Chem. Int. Ed*. **2010**, *49*, 333–336; *Angew. Chem.* **2010**, *122*, 343–346.
[8] a) G. N. Tew, R. W. Scott, M. L. Klein, W. F. DeGrado, *Acc. Chem. Res*. **2010**, *43*, 30–39; b) M. A. Schmitt, B. Weisblum, S. H. Gellman, *J. Am. Chem. Soc*. **2004**, *126*, 6848–6849.
[9] N. P. Chongsiriwatana, J. A. Patch, A. M. Czyzewski, M. T. Dohm, A. Ivankin, D. Gidalevitz, R. N. Zuckermann, A. E. Barron, *Proc. Natl. Acad. Sci. U. S. A.* **2008**, *105*, 2794–2799.
[10] C. Toniolo, M. Crisma, F. Formaggio, C. Peggion, *Peptide Sci*. **2001**, *60*, 396-419.
[11] J. Venkatraman, S. C. Shankaramma, P. Balaram, *Chem. Rev*. **2001**, *101*, 3131-3152.
[12] M. De Poli, M. De Zotti, J. Raftery, J. A. Aguilar, G. A. Morris, J. Clayden, *J. Org. Chem.* **2013,** *78*, 2248-2255.
[13] C. M. Venkatachalam, *Biopolymers* **1968**, *6*, 1425-1436.
[14] a) J. E. Jones, V. Diemer, C. Adam, J. Raftery, R. E. Ruscoe, J. T. Sengel, M. I. Wallace, A. Bader, S. L. Cockroft, J. Clayden, S. J. Webb, *J. Am. Chem. Soc*. **2016**, *138*, 688–695; b) S. J. Pike, J. E. Jones, J. Raftery, J. Clayden, S. J. Webb, *Org. Biomol. Chem*. **2015**, *13*, 9580-9584.
[15] C. Adam, A. D. Peters, M. G. Lizio, G. F. S. Whitehead, V. Diemer, J. A. Cooper, S. L. Cockroft, J. Clayden, S. J. Webb, *Chem. Eur. J.* **2018**, *24*, 2249-2256.
[16] J. K. Chugh, B. A. Wallace, *Biochem. Soc. Trans*. **2001**, *29*, 565-570.
[17] R. Schweitzer-Stenner, J. B. Soffer, S. Toal, D. Verbaro in *Intrinsically Disordered Protein Analysis: Volume 1, Methods and Experimental Tools*, (Eds.: N. V. Uversky, K. A. Dunker), Humana Press: Totowa, NJ, **2012**; pp. 315-346.
[18] R. A. G. D. Silva, S. C. Yasui, J. Kubelka, F. Formaggio, M. Crisma, C. Toniolo, T. A. Keiderling, *Biopolymers*, **2002**, *65*, 229-243.
[19] C. Toniolo, G. M. Bonora, V. Barone, A. Bavoso, E. Benedetti, B. Di Blasio, P. Grimaldi, F. Lelj, V. Pavone, C. Pedone, *Macromolecules*, **1985**, *18*, 895-902.
[20] D. F. Kennedy, M. Crisma, C. Toniolo, D. Chapman, *Biochemistry*, **1991**, *30*, 6541-6548.
[21] A. Barth, *Biochim. Biophys. Acta, Bioenerg.* **2007**, *1767*, 1073-1101.
[22] N. C. Maiti, M. M. Apetri, M. G. Zagorski, P. R. Carey, V. E. Anderson, *J. Am. Chem. Soc*. **2004**, *126*, 2399-2408.
[23] D. M. Byler, H. Susi, *Biopolymers* **1986**, *25*, 469-487.
[24] M. Crisma, W. Bisson, F. Formaggio, Q. B. Broxterman, C. Toniolo, *Biopolymers* **2002**, *64*, 236-245.
[25] C. Toniolo, E. Benedetti, *Trends Biochem. Sci.* **1991,** *16*, 350-353.
[26] R. O. Fox, F. M. Richards, *Nature* **1982**, *300*, 325–330.
[27] C. L. North, M. Barranger-Mathys, D. S. Cafiso, *Biophys. J.* **1995**, *69*, 2392-2397.
[28] E. S. Salnikov, M. De Zotti, F. Formaggio, X. Li, C. Toniolo, J. D. J. O'Neil, J. Raap, S. A. Dzuba, B. Bechinger, *J. Phys. Chem. B*, **2009**, *113*, 3034-3042.
[29] M. Bak, R. P. Bywater, M. Hohwy, J. K. Thomsen, K. Adelhorst, H. J. Jakobsen, O. W. Sørensen, N. C. Nielsen, *Biophys. J.* **2001**, *81*, 1684-1698.
[30] R. A. G. D. Silva, J. Kubelka, P. Bouř, S. M. Decatur, T. A. Keiderling, *Proc. Natl. Acad. Sci. U.S.A.* **2000**, *97*, 8318-8323.
[31] J. Kubelka, R. A. G. D. Silva, T. A. Keiderling, *J. Am. Chem. Soc*. **2002**, *124*, 5325–5332.
[32] C. Toniolo, F. Formaggio, S. Tognon, Q. B. Broxterman, B. Kaptein, R. Huang, V. Setnicka, T. A. Keiderling, I. H. McColl, L. Hecht, L. D. Barron, *Biopolymers* **2004**, *75*, 32-45.
[33] C. R. Jacob, *ChemPhysChem* **2011**, *12*, 3291-3306.
[34] a) R.-P. Hummel, C. Toniolo, G. Jung, *Angew. Chem. Int. Ed*., **1987**, *26*, 1150-1152; *Angew. Chem*. **1987**, *99*, 1180–1182; b) J. Solà, G. A. Morris, J. Clayden *J. Am. Chem. Soc*. **2011**, *133*, 3712-3715.
[35] M. De Poli, L. Byrne, R. A. Brown, J. Solà, A. Castellanos, T. Boddaert, R. Wechsel, J. D. Beadle, J. Clayden *J. Org. Chem.* **2014**, *79,* 4659–4675.
[36]. R. A. Brown, T. Marcelli, M. De Poli, J. Solà, J. Clayden, *Angew. Chemie Int. Ed*. **2012**, *51*, 1395-1399; *Angew. Chem*. **2012**, *124*, 1424–1428.
[37] S. J. Pike, J. Raftery, S. J. Webb, J. Clayden, *Org. Biomol. Chem*. **2014**, *12*, 4124-4131.
[38]. J. Solà, M. Helliwell, J. Clayden, *Biopolymers* **2011**, *95*, 62-69.
[39] S. J. Pike, V. Diemer, J. Raftery, S. J. Webb, J. Clayden, *Chem. Eur. J.* **2014**, *20*, 15981–15990.
[40] S. C. Yasui, T. A. Keiderling, F. Formaggio, G. M. Bonora, C. Toniolo, *J. Am. Chem. Soc*. **1986**, *108*, 4988-4993.
[41] A. N. L. Batista, J. M. Batista Jr, V. S. Bolzani, M. Furlan, E. W. Blanch, *Phys. Chem. Chem. Phys.* **2013,** *15*, 20147-20152.
[42] H. Balaram, M. Sukumar, P. Balaram, *Biopolymers* **1986**, *25*, 2209-2223.
[43] M. Bellanda, E. Peggion, R. Bürgi, W. van Gunsteren, S. Mammi, *J. Pept. Res*. **2001**, *57*, 97-106.
[44] H. Yurtseven, W. F. Sherman, *J. Mol. Struct.* **1988,** *175*, 465-470.
[45] H. Susi, D. M. Byler, *Appl. Spectrosc*. **1988**, *42*, 819-826.
[46] L. D. Barron, L. Hecht, *Structure and Behavior of Biomolecules from Raman Optical Activity. In Comprehensive Chiroptical Spectroscopy*, John Wiley & Sons, Inc.: **2012**; pp 759-793.
[47] G. Zajac, A. Kaczor, S. Buda, J. Młynarski, J. Frelek, J. C. Dobrowolski, M. Baranska, *J. Phys. Chem. B*, **2015,** *119*, 12193-12201.
[48] C. Merten, L. D. Barron, L. Hecht, C. Johannessen, *Angew. Chem. Int. Ed.* **2011,** *50*, 9973-9976; *Angew. Chem.* **2011**, *123*, 10149-10152.
[49] A. Rygula, K. Majzner, K. M. Marzec, A. Kaczor, M. Pilarczyk, M. Baranska, *J. Raman Spectrosc.* **2013,** *44*, 1061-1076.
[50] G. Zhu, X. Zhu, Q. Fan, X. Wan, *Spectrochim. Acta, Part A*, **2011,** *78*, 1187-1195.
[51] R. C. Lord, N.-T. Yu, *J. Mol. Biol.* **1970,** *50*, 509-524.
[52] J. De Gelder, K. De Gussem, P. Vandenabeele, L. Moens, *J. Raman Spectrosc.* **2007,** *38*, 1133-1147.
[53] L. D. Barron, E. W. Blanch, I. H. McColl, C. D. Syme, L. Hecht, K. Nielsen, *Spectroscopy* **2003,** *17*, 101-126.
[54] L. D. Barron, L. Hecht, E. W. Blanch, A. F. Bell, *Prog. Biophys. Mol. Biol.* **2000,** *73*, 1-49.
[55] a) J. Kubelka, R. Huang, T. A. Keiderling, *J. Phys. Chem. B*, **2005**, *109*, 8231-8243; b) T. A. Keiderling, R. A. G. D. Silva, G. Yoder, R. K. Dukor, *Bioorg. Med. Chem*. **1999**, *7*, 133-141.

WILEY-VCH

[56] a) P. Barton, C. A. Hunter, T. J. Potter, S. J. Webb, N. H. Williams, *Angew. Chem. Intl. Ed.* **2002**, *41* 3878-3881; *Angew. Chem.* **2002**, *114*, 4034–4037; b) M. J. Langton, F. Keymeulen, M. Ciaccia, N. H. Williams, C. A. Hunter, *Nature Chem*, **2017**, *9*, 426-430; c) M. J. Langton, N. H. Williams, C. A. Hunter, *J. Am. Chem. Soc*. **2017**, *139*, 6461-6466; d) M. J. Langton, L. M. Scriven, N. H. Williams, C. A. Hunter, *J. Am. Chem. Soc*. **2017**, *139*, 15768–15773.

[57] D. E. Warschawski, A. A. Arnold, M. Beaugrand, A. Gravel, É. Chartrand, I. Marcotte, *Biochim. Biophys. Acta, Biomembr.* **2011**, *1808*, 1957–1974.

[58] T. Nagao, D. Mishima, N. Javkhlantugs, J. Wang, D. Ishioka, K. Yokota, K. Norisada, I. Kawamura, K. Ueda, A. Naito, *Biochim. Biophys. Acta, Biomembr*. **2015**, *1848*, 2789–2798.

[59]. a) C. Zhao, P. L. Polavarapu, *Biopolymers*, **2001**, *62*, 336–340; b) P. Novotná, M. Urbanová, *Anal. Biochem*. **2012**, *427*, 211–218; c) P. Novotná, I. Goncharova, M. Urbanová, *Biochim. Biophys. Acta*, **2014**, *1838*, 831–841; d) L. Kocourková, P. Novotná, L. Šťovíčková-Habartová, S. Čujová, V. Čeřovský, M. Urbanová, V. Setnička, *Monatsh. Chem*., **2016**, *147*, 1439-1445; e) L. Kocourková, P. Novotná, S. Čujová, V. Čeřovský, M. Urbanová, V. Setnička, *Spectrochim. Acta A*, **2017**, *170*, 247-255; f) D. Das, S. Kumar Pal, *ChemistrySelect*, **2017**, *2*, 4779 – 4786.

[60] M. Jackson, H. H. Mantsch, *Crit. Rev. Biochem. Mol. Biol.* **1995**, *30*, 95-120.

[61] M. Tomsett, I. Maffucci, B. A. F. Le Bailly, L. Byrne, S. M. Bijvoets, M. G. Lizio, J. Raftery, C. P. Butts, S. J. Webb, A. Contini, J. Clayden, *Chem. Sci*. **2017**, *8*, 3007-3018.

[62] P. H. C. Eilers, H. F. M. Boelens, *Baseline correction with asymmetric least squares smoothing*, Leiden University Medical Centre report, **2005**.

WILEY-VCH

Entry for the Table of Contents

FULL PAPER

The turn of the screw: Raman optical activity (ROA) and vibrational circular dichroism (VCD) spectroscopies of helical α-aminoisobutyric acid foldamers have provided chiroptical signatures for both left- and right-handed 3_{10}-helices in organic solvents, with VCD indicating that foldamer screw-sense is preserved when the foldamers are embedded in bilayers.

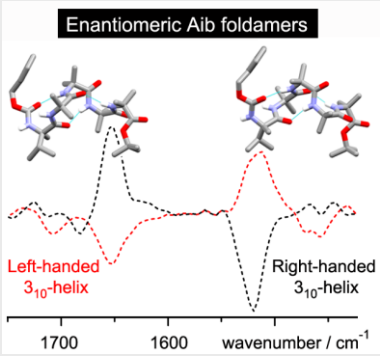

Maria Giovanna Lizio, Valery Andrushchenko, Sarah J. Pike, Anna D. Peters, George F. S. Whitehead, Iñigo J. Vitórica-Yrezábal, Shaun T. Mutter, Jonathan Clayden, Petr Bouř, Ewan W. Blanch,* and Simon J. Webb**

Page No. – Page No.

Optically-Active Vibrational Spectroscopy of α-Aminoisobutyric Acid Foldamers in Organic Solvents and Phospholipid Bilayers

WILEY-VCH